June 2006 seismic swarm and dike emplacement event beneath the Michoacan-Guanajuato volcanic field, Mexico

Tiffany F. Cox

Senior Integrative Exercise

March 11, 2009

Submitted in partial fulfillment of the requirements for a Bachelor of Arts degree from Carleton College, Northfield, Minnesota.

TABLE OF CONTENTS

June 2006 seismic swarm and dike emplacement event beneath the Michoacan-Guanajuato volcanic field, Mexico

Tiffany Cox
Carleton College
Senior Integrative Exercise
March 11, 2009

Advisors:
Sarah Titus, Carleton College
Mike West, University of Alaska, Fairbanks

ABSTRACT

In June 2006, a seismic swarm was recorded 15 km from the summit of the cinder cone Paricutin in the Michoacan-Guanajuato volcanic field in central Mexico. The 700 earthquakes in the swarm ranged in magnitude from 2.5 to 3.5. Hypocenters were computed for 323 of these events to look for spatial and temporal patterns within the swarm. First motions of each event were examined and focal mechanisms were calculated for 117 of the relocated events. The relocated hypocenters clearly show a shallowing trend with time and no consistent focal mechanism solutions. I suggest that the swarm was related to a dike emplacement event. The seismic data indicate a period of vertical migration (200 m/day) coupled with a northward lateral migration (130 m/day) which I interpret as magma being injected upwards in the crust. Following this injection, there is a period of earthquakes, all occurring at approximately 5 km in depth, which migrated southwards at 100 m/day, indicating a lateral extension of the magma to the south.

Keywords: seismicity, swarm, dikes, emplacement, Michoacan-Guanajuato volcanic field, Mexico

INTRODUCTION

Typical earthquake sequences in plate boundary settings include a main shock followed by aftershocks decreasing in magnitude or a set of foreshocks of increasing magnitude leading up to a large main shock (Mogi, 1963; Shlien and Nafi Toksoz, 1970; Rikitake, 1975; Kanamori, 1981). However, some earthquakes do not obey these patters and instead occur in swarms of similar magnitude and location over a discrete period of time without any large main shocks (Mogi, 1963; Sykes, 1970; Hill, 1977).

Seismic swarms are interpreted to be caused by either tectonic or magmatic events. Tectonic swarms often occur along continental margins, particularly in active rift zones, such as in Africa or the southwestern US (e.g. Pacheco et al., 1999a; Ibs-von Seht et al., 2008)these swarms are typically along a single fault or fracture, in an area where the fault is weaker and slip occurs at lower stress (e.g. Legrand et al., 2002; Ibs-von Seht et al., 2008; Kiratzi et al., 2008). Magmatic swarms or associated with motion of magma in the subsurface, such as a dike injection or a precursor to volcanic eruption (e.g. Hill et al., 1990; Newman et al., 2001; Toda et al., 2002; Pederson et al., 2007)

In this study, I investigate the spatial and temporal characteristics of an earthquake swarm in central Mexico. Because the swarm is located near both an active rift zone and a volcanic field, either a tectonic solution or magmatic solution is possible. Based on the migratory behavior of the earthquakes and the lack of consistent focal mechanisms, I suggest the swarm is magmatic, most likely associated with a dike intrusion.

TRANS-MEXICAN VOLCANIC BELT

The Trans-Mexican Volcanic Belt is a 1200-km-long volcanic chain that extends from the Pacific Ocean to the Gulf of Mexico (Fig. 1). Volcanism began in central Mexico in the Miocene due to oblique subduction of the Rivera and Cocos plates within a transtensional environment (Ferrari et al., 1994; Ferrari et al., 2000). Presently, volcanism is affected by two tectonic regimes: subduction of the Rivera offshore and intracontinental rifting. Subduction of the Rivera and Cocos plates is oblique but not parallel, resulting in collision of the slabs in the subsurface (Ferrari et al., 2000). The intraplate rifting is centered in the Guadalajara district, and is bounded by the Jalisco and Michoacan blocks to the west and east (Ferrari et al., 1994). Rifting has alternately been attributed to a relocation of the East Pacific Rise (Luhr et al., 1985), the presence of a hotspot (Moore et al., 1994), or passive rifting due to the oblique motion occurring within the subduction zone (Ferrari et al., 1994).

This study focuses on the central segment of the Trans-Mexican Volcanic Belt known as the Michoacan-Guanajuato Volcanc Field (Fig. 2; Macias, 2007). Volcanism in this region is characterized by both shield volcanoes and monogenetic cinder cones, with magmatic compositions ranging from basaltic to basaltic andesite (Hasenka and Carmichael, 1985; Gomez-Tuena et al., 2007). This volcanic field is located to the east of the Colima rift zone and includes over 1400 volcanoes (Rosas-Elguera et al., 1996). The most recent volcanic event was the continuous eruption of Volcan de Paricutin from 1943 to 1958. Paricutin is classified as a monogenetic cinder cone, of relatively uniform olivine basaltic composition, which opened spewing small ash clouds and lava from a farmer’s field (Krauskopf, 1948; Hasenka and Carmichael, 1985).

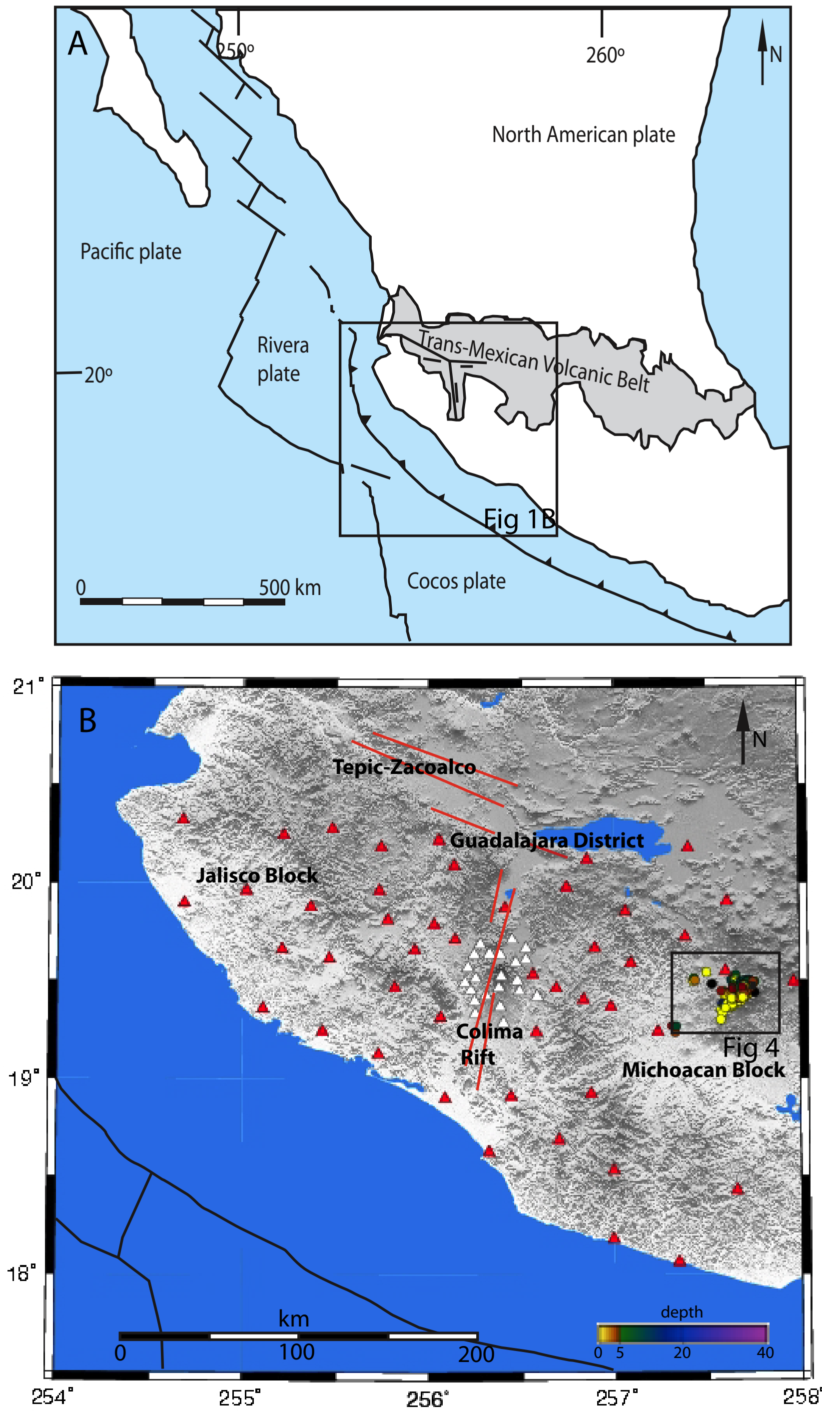

Figure 1. Location maps **(A)** shows the location of the Trans-Mexican Volcanic Belt within the regional tectonics (Modified from Ferrari et al., 2000). Map in **(B)** is closer view of study area with the stations array. The inset box shows the position of the seismic swatm in the Michoacan-Guanajuato Volcanic Field. Red triangles are stations of the MARS array. White triangles are stations of the CODEX array. Dots are individual events. Earthquake depths are in km.

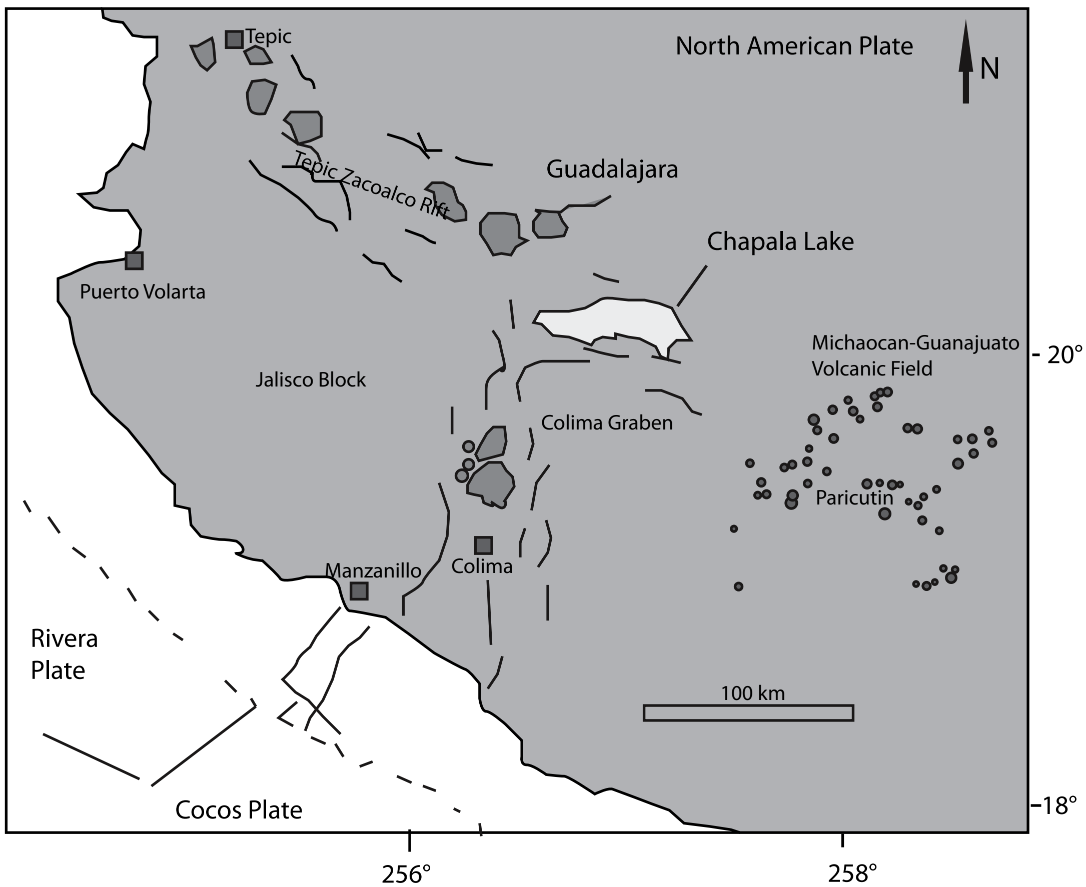

Figure 2. Map of field area. Each dot represents a volcano within the Michoacan-Guanajuato volcanic field. Darker shaded regions are Miocene lava flows located within the rift zone (modified from Macias, 2007).

The majority of seismicity within the region is caused by the subduction off shore, and events become deeper farther from the plate boundary. Other seismic events within the area are often associated with rifting and volcanism; both magmatic and tectonic earthquake swarms have been previously documented (Pacheco et al., 1999a; Pacheco et al., 1999b).

SEISMICITY AND EARTHQUAKE LOCATION

Data Collection

The earthquake data from this study were collected from two seismic arrays: the Mapping the Rivera Subduction Zone (MARS) and the Colima Volcano Deep Seismic Experiment (CODEX) arrays (Fig. 1). These arrays were deployed during January 2006 and were intended to collect data for 24 months, although the scientific focus of each deployment was different. The MARS array was designed to determine the behavior of the subduction zone using p-wave tomography (Grand et al., 2007). The CODEX array was designed to probe the deep magmatic structure of the volcanic center of Colima Volcano (Gardine et al., 2007).

The swarm of earthquakes considered in this study includes 700 events that occurred between May 28 and July 2, 2006, and range in magnitude from 2.5 to 3.5. These earthquakes are of interest for three reasons. First, they are located near Volcan de Paricutin, the last volcano to erupt within the region. Second, although these events represent a very small fraction of the observed seismicity, they are located east of the major seismicity associated with rifting. Third, these events are all relatively shallow (5-9 km) whereas seismicity associated with the Cocos subduction zone would be expected to be much deeper at this distance from the plate boundary.

Data processing

P- and S- wave arrival times were picked automatically from each earthquake above a minimum magnitude (M_w) of 2.5 based on waveforms (Fig. 3). To improve the dataset, I repicked arrival times for 323 of the events by, in order to add more parameters for finding event hypocenters. Based on time constraints, I filtered the data from the second half of the swarm by only allowing events with 30 or more automated picks, on 15 or more stations.

I used the program Antelope to find hypocenter locations based on available waveforms. Using arrival times from a minimum of 15 stations, the program traces probable travel paths, and the point of maximum path intersection was defined as the original hypocenter location. These hypocenters vary from 0-15 km and are distributed on the northern and western flanks of Paricutin (Fig. 4A).

I used the program hypoDD to perform a double difference relocation algorithm on the hypocenters. This method is very common for earthquake analyses (Brown et al., 2004; Mandal and Horton, 2007; Dunn et al., 2008; von Seggern et al., 2008). The method minimizes the path error by connecting different events to one another (Waldhauser and Ellsworth, 2000).The algorithm used by hypoDD correlates events into clusters, discarding anomalous events separated spatially from the main cluster (Waldhauser and Ellsworth, 2000). Six events were disregarded based on a separation of time and space from the main duration of the swarm. Relocated hypocenters collapse into a narrow 5 km long band a few km northwest of Volcan de Paricutin (Fig. 4B).

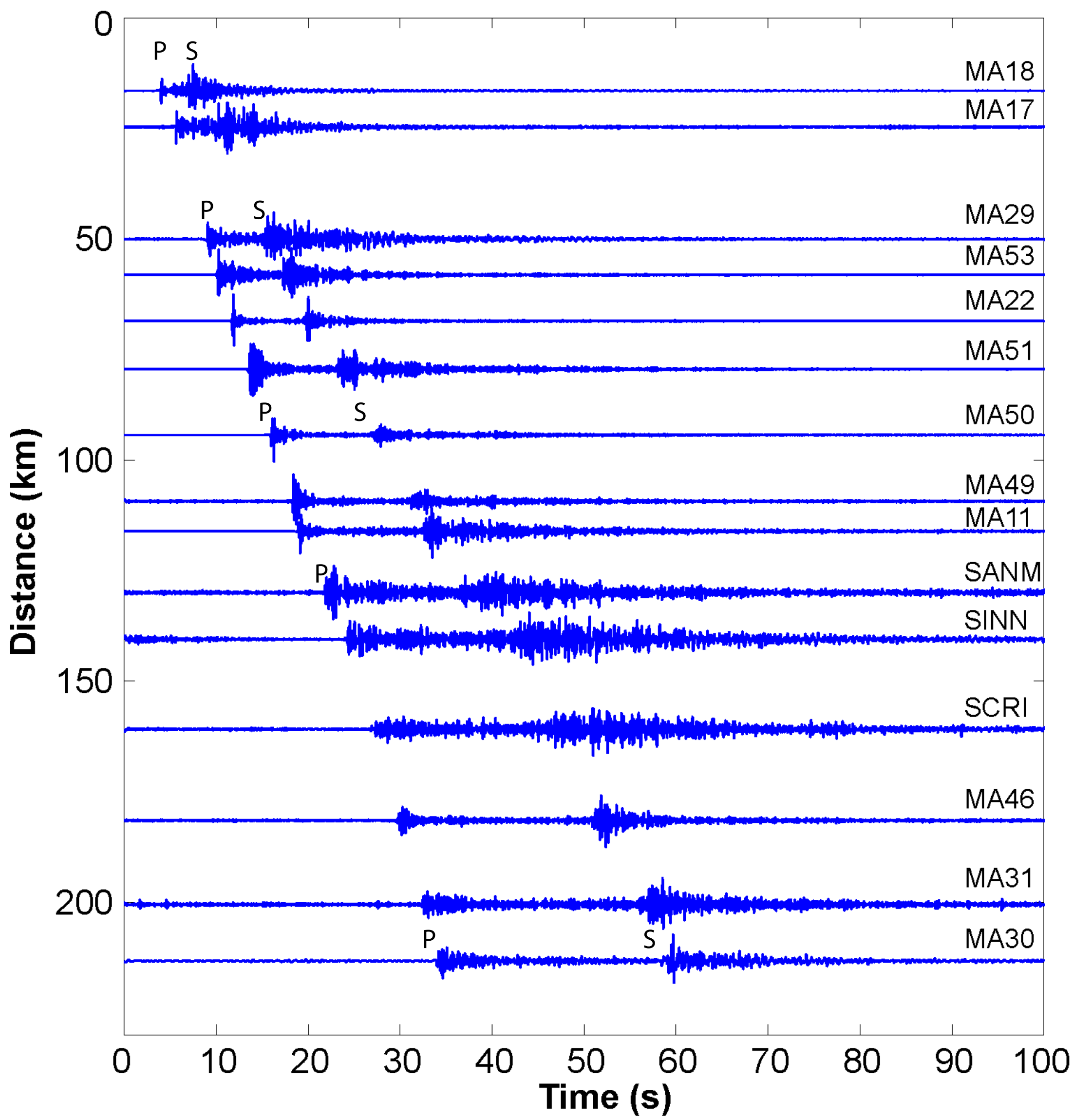

Figure 3. Record-section plot of an ML 3.3 earthquake on June 11, 2006 located in the Michoacan-Guanajuato volcanic field as recorded by stations in the MARS and CODEX arrays. Vertical components of waveforms only.

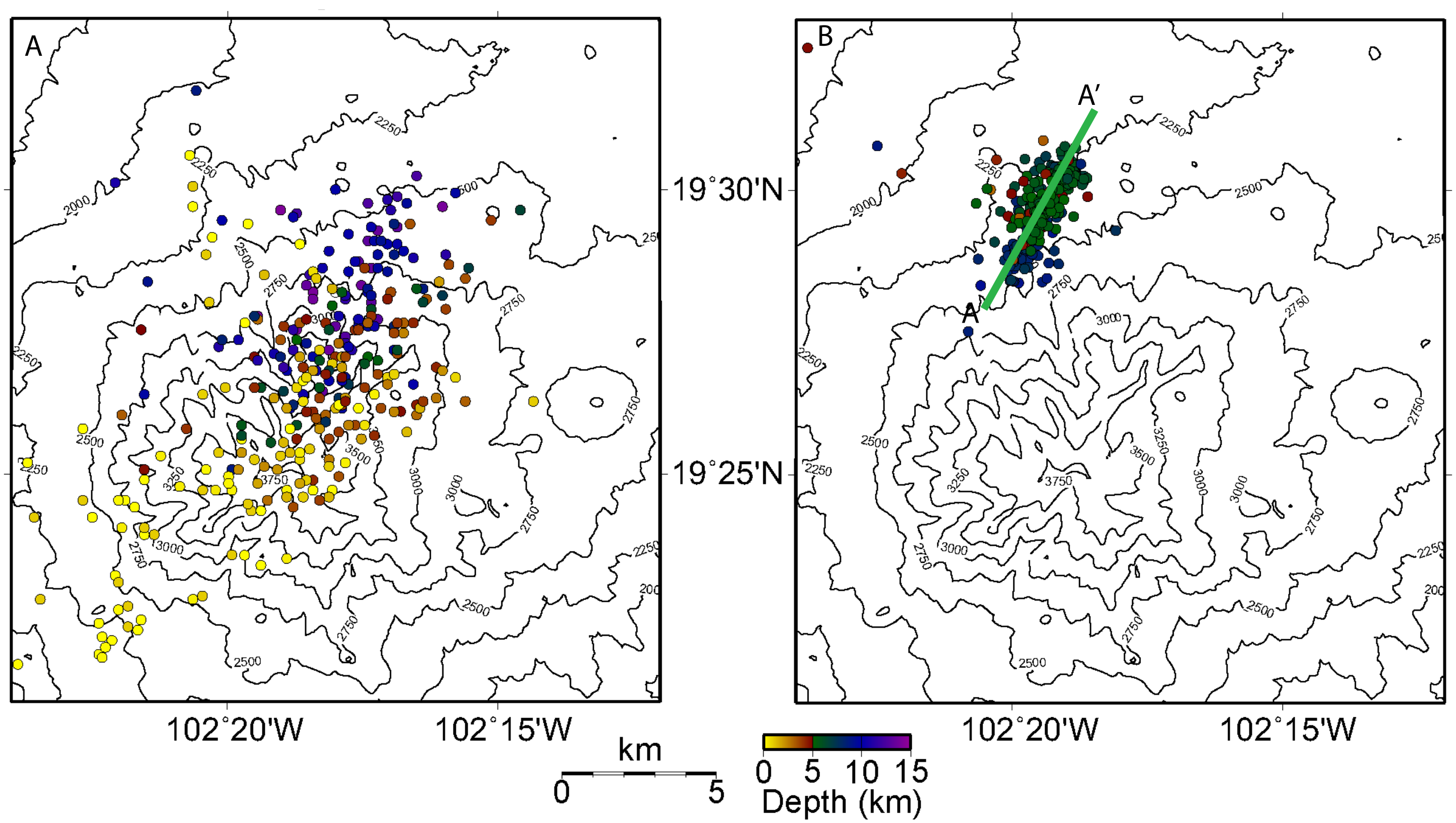

Figure 4. Map of **(A)** original and **(B)** relocated hypocenters. Note the collapse of the distribution for the relocated hypocenters. Cross-section across **(B)** relocations correlates to Figure 6.

To test the reliability of relocted hypocenters, I did several trials with different parameters, varying the maximum allowed number of correlations between events, as well as the maximum number of neighboring events to consider. Unless large variations are made to several of the parameters, the algorithm yields the similar results. Because of this, I feel confident in the relocated hypocenters which are used for the remainder of this study.

SPATIAL AND TEMPORAL EARTHQUAKE ANALYSIS

To better understand the positions of hypocenters during the swarm, I have plotted latitude vs. time in Figure 5A and depth vs. time in Figure 5B. From May 28 to May 31, there is a small period of increasing seismicity at 9 km depth, towards the southern tip of the swarm. From June 1 to June 12, the hypocenter locations migrate north and upward. After June 12, the upward migration ceases, with the earthquakes remaining at a depth of 5 km; the lateral migration reverses, and the hypocenter locations migrate back to the south. This behavior occurs from June 13 to July 2, at which point in time the swarm ceases.

To summarize, the swarm is separated into three stages of activity, separated in time and depth. These stages, referred to as stages I, II, and III, are illustrated schematically in Figure 6 which links time and depth by projecting Figure 5 onto the cross-section. Stage I correlates to the beginning of the swarm, Stage II refers to the upward migration, and Stage III marks the final period of the swarm, where the depths stay centralized and there is only lateral migration.

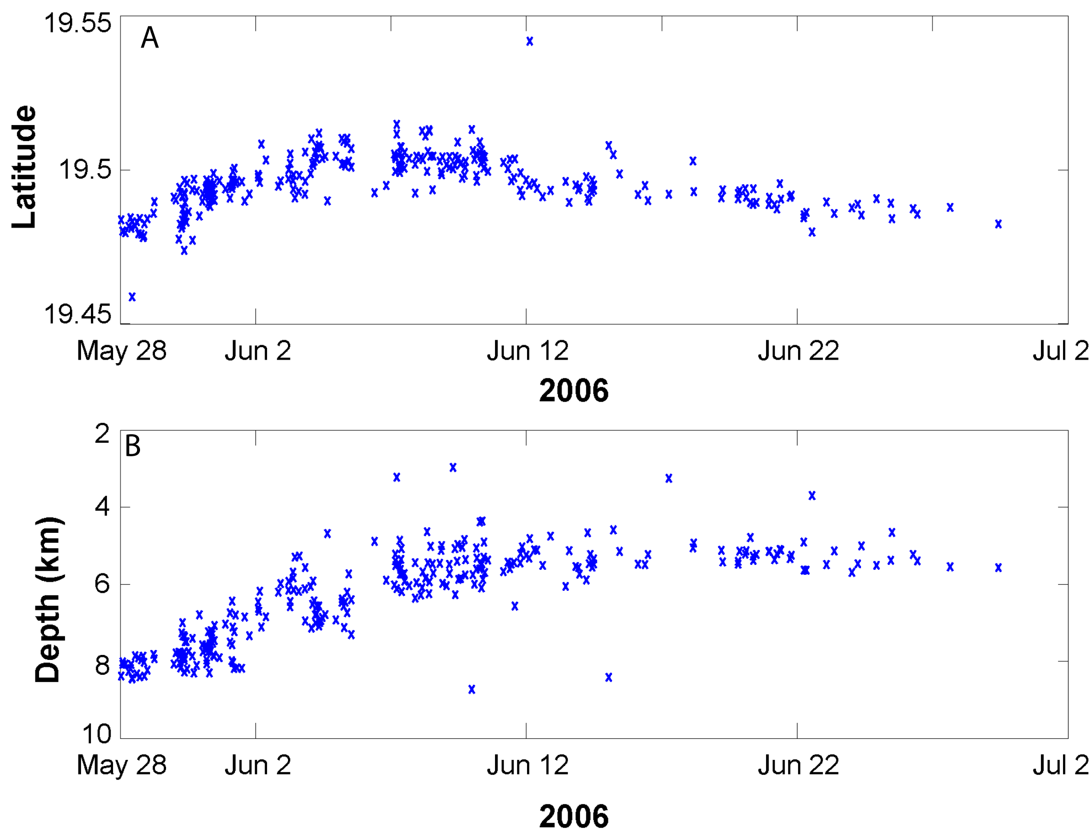

Figure 5. Plots of events at latitude position **(A)** and depth **(B)** versus time. Note migratory patterns which arise in both plots.

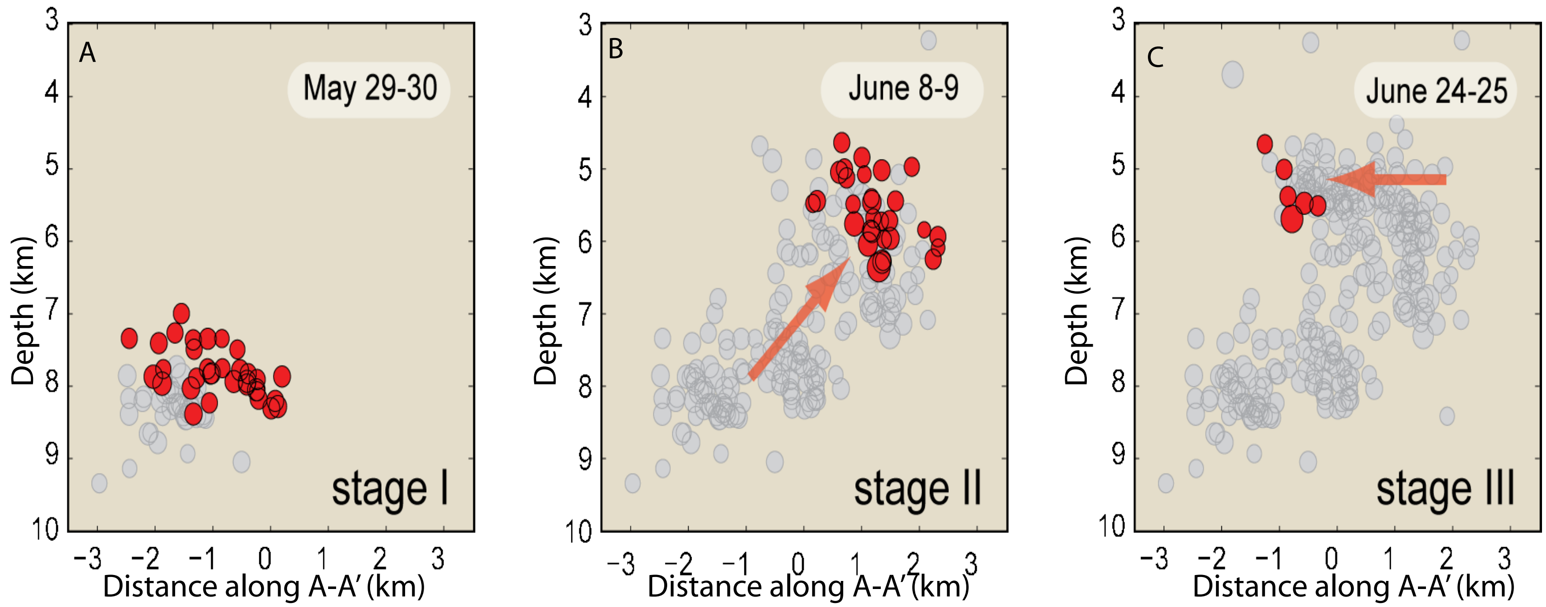

Figure 6. Hypocenter migration depicted through both time and space. Stage 1 **(A)** represents the beginning of the swarm, Stage II **(B)** represents the main migration from depth, and Stage III **(C)** represents the final lateral migration

Stage I corresponded to the initiation of the swarm, a period of three days, May 28 to May 31, and is characterized by vigorous deep seismicity (Fig. 6A). These ~ 50 events were located at around 8-9 km of depth and occur prior to any evident spatial migration.

Stage II includes 200 events June 1 to June 12 and is characterized by a spatial and temporal migration occurring both vertically and laterally (Fig. 6B). The hypocenter locations moved up to a depth of ~5 km and laterally traveled 3-4 km to the northeast. Alternatively stated, the vertical rise was ~200 m/day and the horizontal motion was ~ 130 m/day.

Stage III includes ~70 events from June 13 and continued until the termination of the swarm on July 2 (Fig. 6C). The depth remained at a static depth of 5km; but earthquakes moved 2-3 km to the south of those found in Stage II. This southward migration is slower than the initial northward migration, being only about 100m/day.

FOCAL MECHANISM ANALYSIS

Introduction to focal mechanisms

Focal mechanisms are a tool used to study the geometry of possible faulting during an earthquake. Seismic stations which record the event are used to generate data points. Since the hypocenter location is well known, the azimuth and emergence angle are determined based on the distance of each station from the hypocenter. The azimuth is a vector which relates measures the direction of the station away from the hypocenter while the emergence angle is the angle between the wave and an imaginary vertical line just as it exits the hypocenter (Fig. 7; Stein and Wysession, 2003; Cronin, 2004).

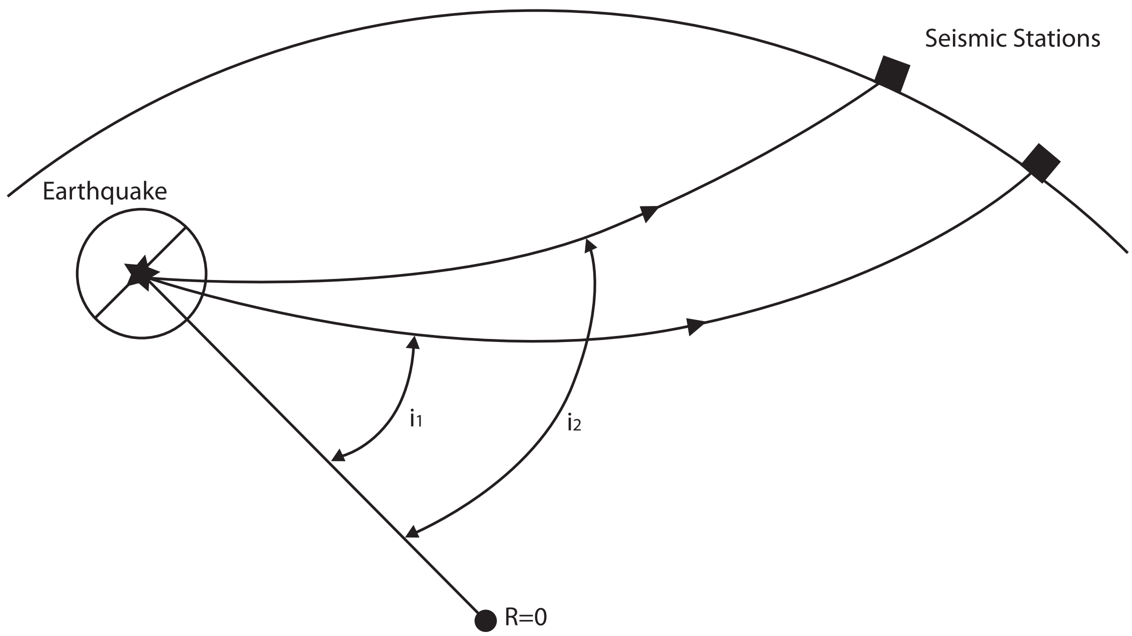

Figure 7. The emergence angle at the earthquake hypocenter is the angle from the vertical at which the wave leaves the hypocenter. This angle varies depending on the seismic station receiving the signal (modified from Stein and Wysession, 2003).

Each data point is also assigned a behavior of either compressional or dilational, depending on the first motion behavior of the vertical seismogram(Stein and Wysession, 2003). A first motion is defined as the polarity, or direction, the first p-wave arrival exhibits. A dilational event will have a first motion where material moves away from the station whereas a compressional event will have material initially move toward the station (Fig. 8; Stein and Wysession, 2003; Cronin, 2004).

From these data, the possible fault solutions can be determined. The most common focal mechanism solutions are called double-couple focal mechanisms with two nodal planes (Fig. 9). These nodal planes represent the possible fault solutions, and based on the data, either configuration is likely (Cronin, 2004). Focal mechanisms may also have a non-double-couple solution, whose nodal surfaces do not plot as planes. In order to fully explain these focal mechanisms, another data source, in addition to P-wave polarities, is necessary, such as an examination of wave amplitudes (Frohlich et al., 1989; Frohlich, 1994; Miller et al., 1998). Examples of non-double-couple focal mechanisms are shown in Figure 10.

Within these focal mechanisms there are also axes which represent the principal maximum and minimum stress, or amount of force exerted over an area, on the system. These axes, called the P (compressional) and T (tensional), plot on the stereonet halfway between the poles of the nodal planes. The T axis falls in the compressional quadrant and the P axis falls in the dilational quadrant (Cronin, 2004).

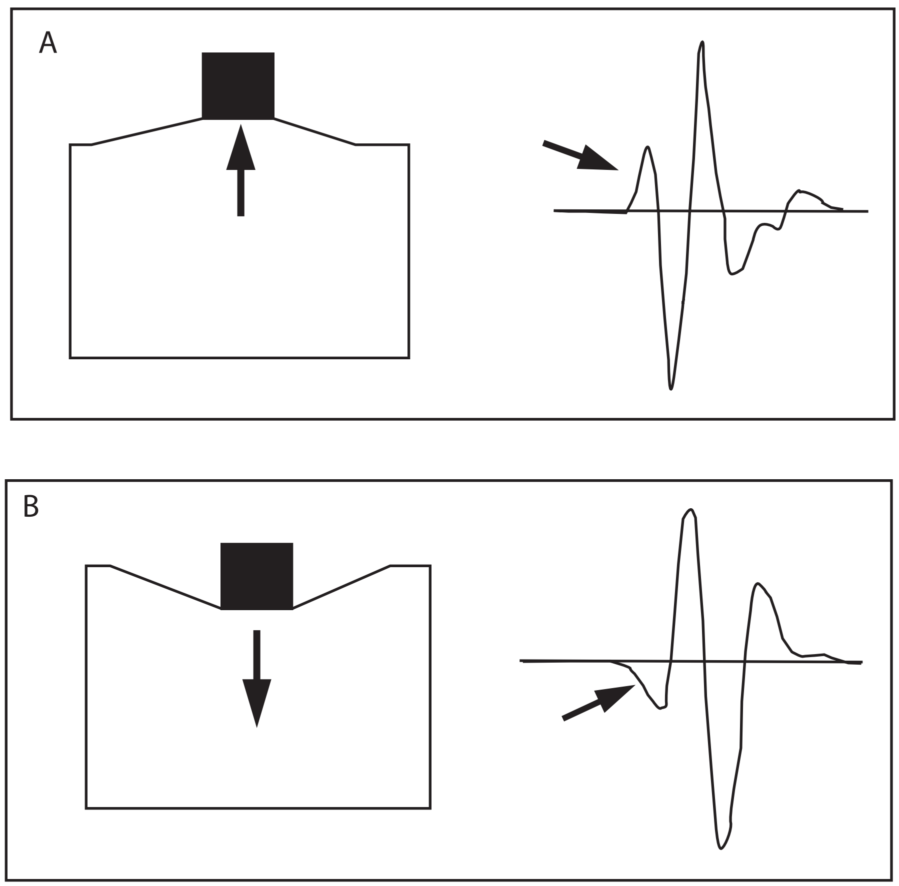

Figure 8. For an event with a compressional first motion **(A)**, the station is initially pushed vertically upwards, which corresponds to a positive peak on the seismogram, wheras for an event with a dilational first motion **(B)**, the station is intially pulled vertically downwards, corresponding to a negative peak on the seismogram.

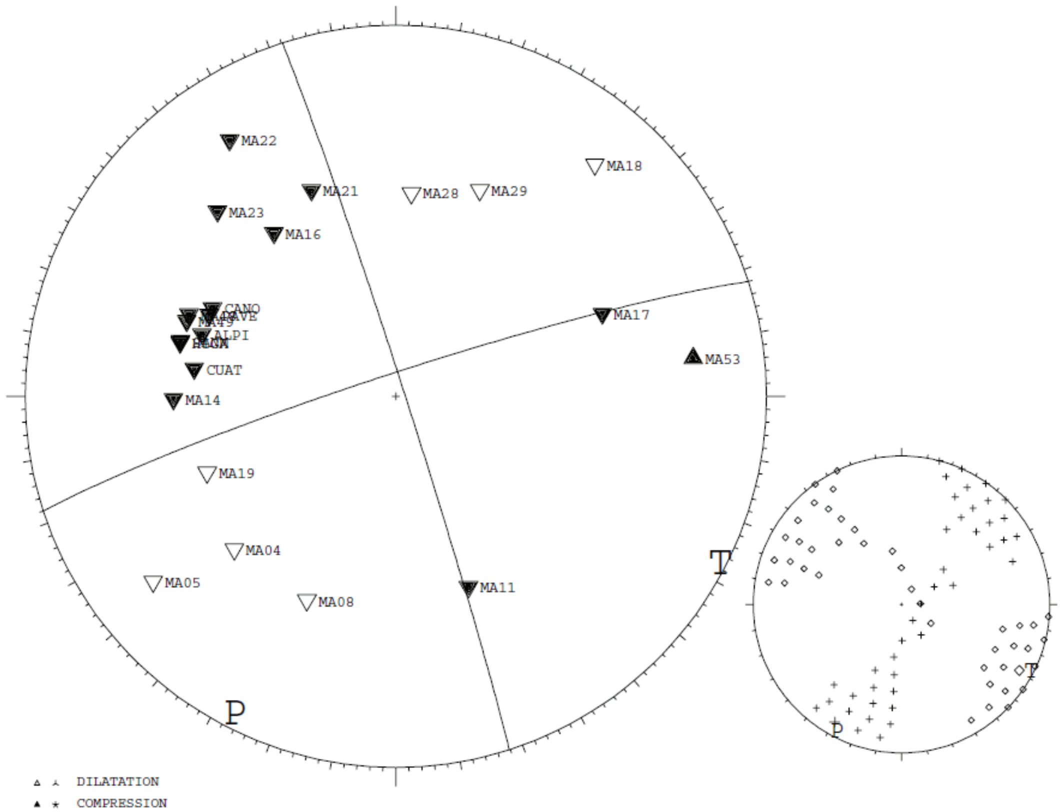

Figure 9. A sample focal mechanism solution derived from fpfit. Each point represents the behavior of the event at a station. Black triangles represent compression, or stations where the first motion felt by the p-wave was vertically upwards, and white triangles represent dilation, where the first motion was vertically down. Smaller cricle represents derived stress solutionfor determination of P and T axis placement.

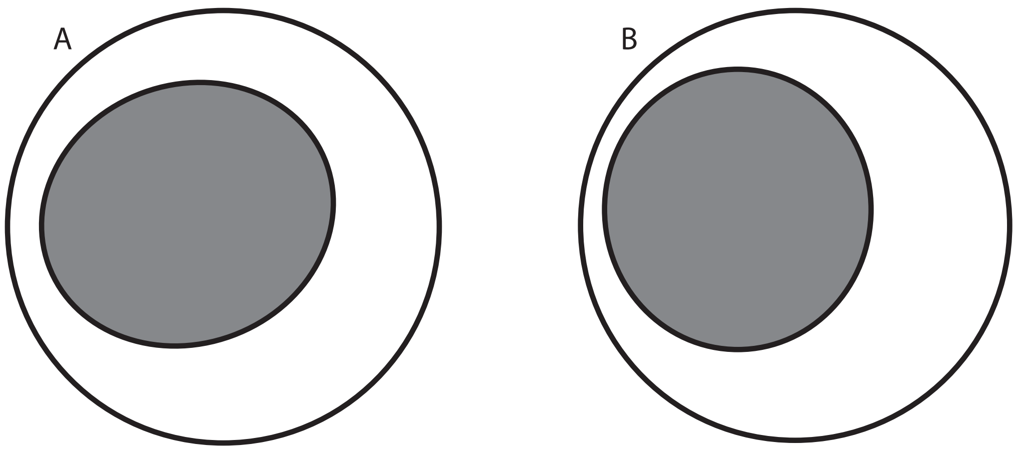

Figure 10. Two possible non-double-couple focal mechanism solutions from first motion behavior which isolates the compressional region (modified from Nettles and Ekstrom, 1998).

Data processing

I determined the first motion of the p-waves at each station for each event. Using fpfit software (Reasenberg and Oppenheimer, 1985), I determined the specific azimuthal projections for each station and correlated it to the emergence angle for each event. These data were inverted to find two nodal planes (Fig. 9). I disregarded events with fewer than ten identifiable first motions and events with a large amount of uncertainty, using only 117 different event focal mechanisms.

Data analysis

Double-couple solutions from fpfit were plotted in map view (Fig. 11). These show no consistent pattern, and solutions for normal, thrust, and strike-slip faulting is evident. No trends are apparent through space, indicating there is not a single fault plane solution which corresponds to this swarm.

In Figure 12, I attempted to locate a pattern of first motions in order to determine a possible non-double-couple focal mechanism. An initial cross-correlation of waveforms indicated possible patterns between events; however, this correlation was done for one station, and did not accurately represent first motion behavior. An attempt to extrapolate across other stations resulted in an extreme lack of consistency. Figure 12 shows the behavior of earthquake first motions for each station through time. The red bars indicate a compressional first motion, and the blue bars indicate a dilational first motion; white space implies no data. While there are patterns evident within specific stations, there is nothing to suggest a non-double-couple composite focal mechanism solution is possible.

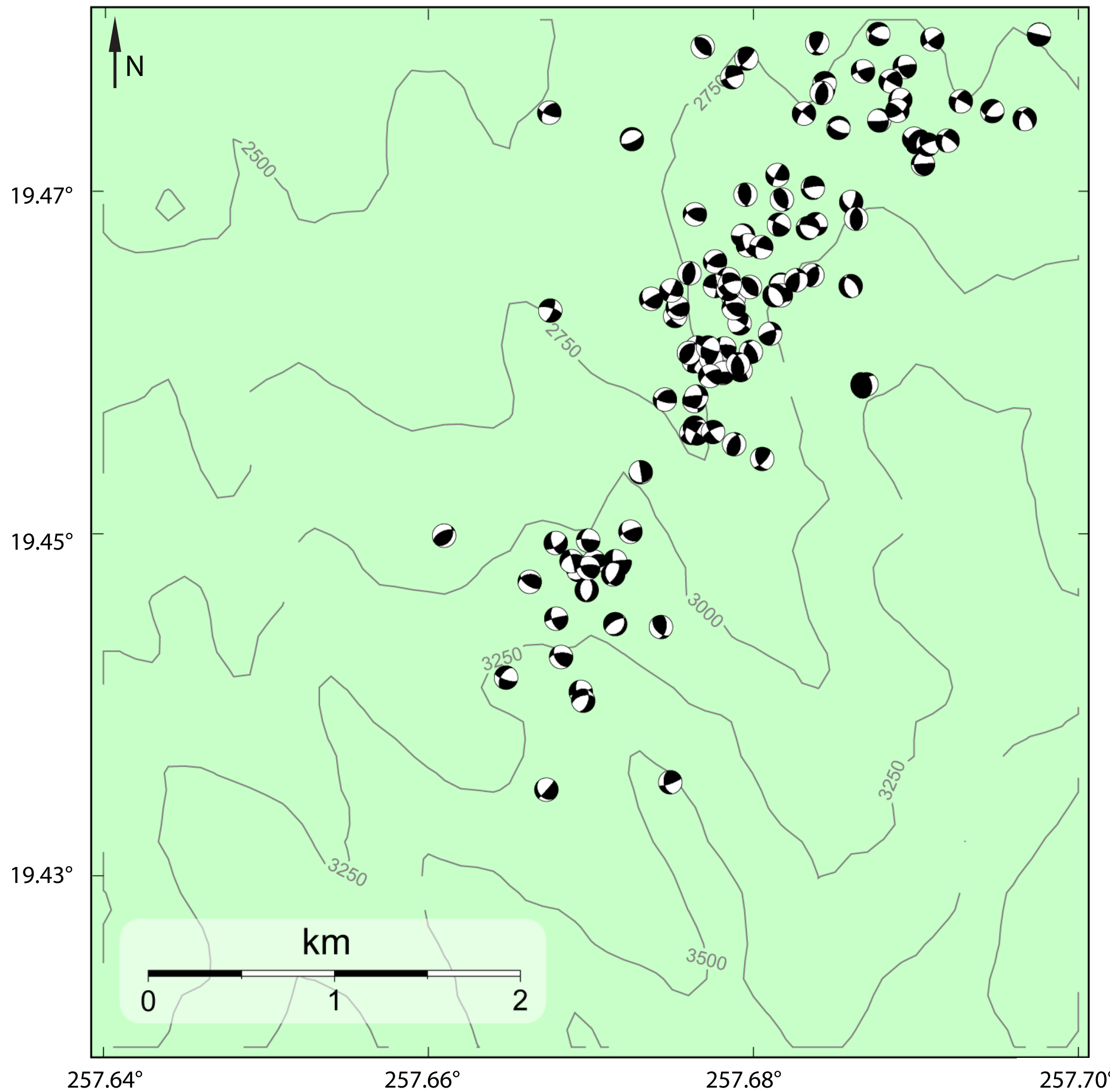

Figure 11. Focal Plane solution for 121 events within the seismic swarm. Note the lack of consistency among focal mechanism solutions, suggesting these events were not caused by slip along a single plane, or fault.

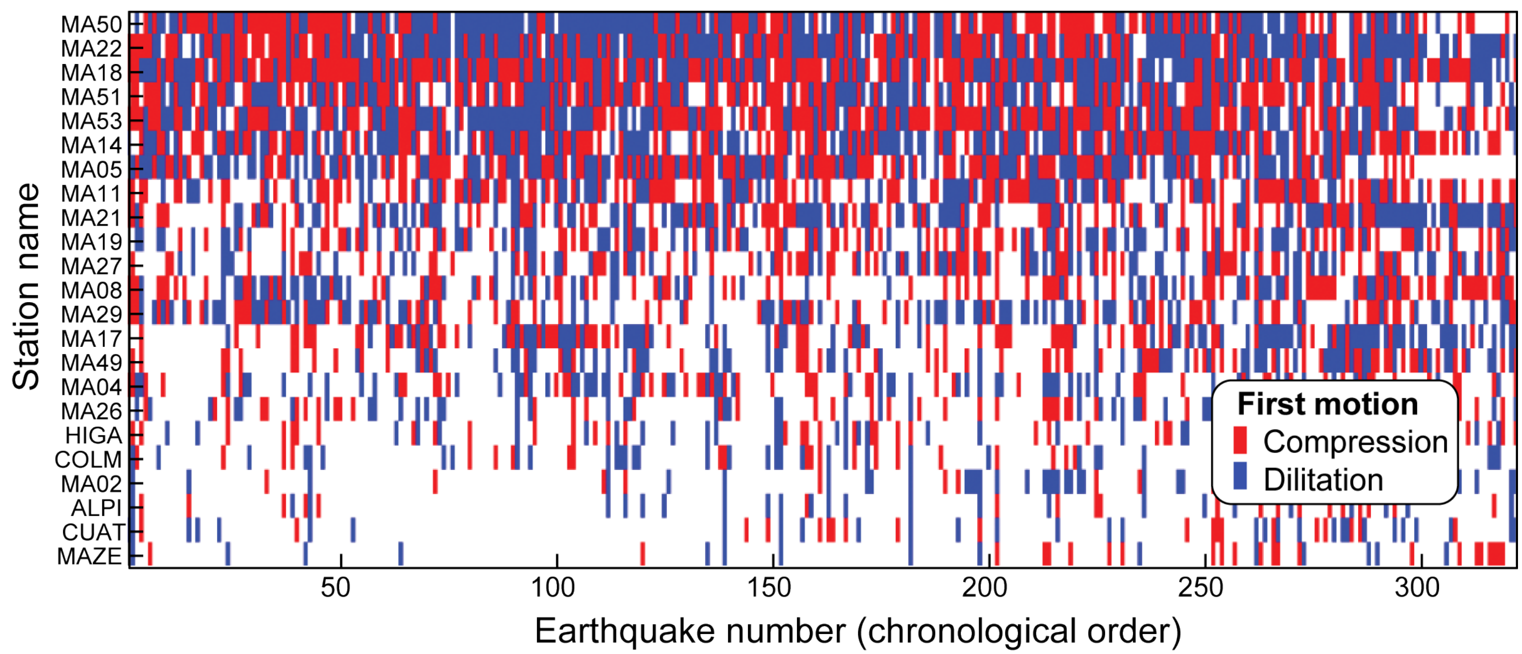

Figure 12. P-wave first motions by station through the swarm. This figure shows the first motion for all events on the most used stations, red point indicating compression, blue points dilation. White space means no data at those points. We see no clear patterns that might indicate a consistent fault orientation. This suggests the events were caused by stress adjustments and fracture in the surrounding crust.

DISCUSSION

When examining the swarm in map view, the swarm can be interpreted as either tectonic or magmatic. The hypocenters of the earthquake swarm show that earthquakes are arranged in a narrow band with a small range of shallow depths (Fig. 4B). The strike direction associated with this band runs perpendicular to the direction of subduction,

A tectonic swarm in this region is likely to follow a band of this nature. The swarm is parallel to rifting and perpendicular to the maximum stress induced by subduction. If there is a fracture being induced by subduction, the fracture would likely open in the south first and move north, fitting in with the suggested spatial and temporal trends. A tectonic focal plane would be defined by focal mechanism solutions with a similar nodal plane and type of faulting (Fig. 13A; Pacheco et al., 1999a).

A magmatic swarm in this region would be located near an area of past or recent volcanism where there is magma in the subsurface. The spatial and temporal nature of the swarm will trend towards the surface as the magma rises. A focal plane solution will have a varied number of focal mechanisms, indicating a more complex earthquake mechanism not related to slip along a single plane (Fig. 13B; Roman et al., 2004).

Because the data has an upward migration and a varied focal plane solution, I interpret this to be a magmatic swarm. Due to the close relation between tectonic and magmatic earthquake swarms in map view, seismic analysis and focal mechanism formulation is essential in making this distinction.

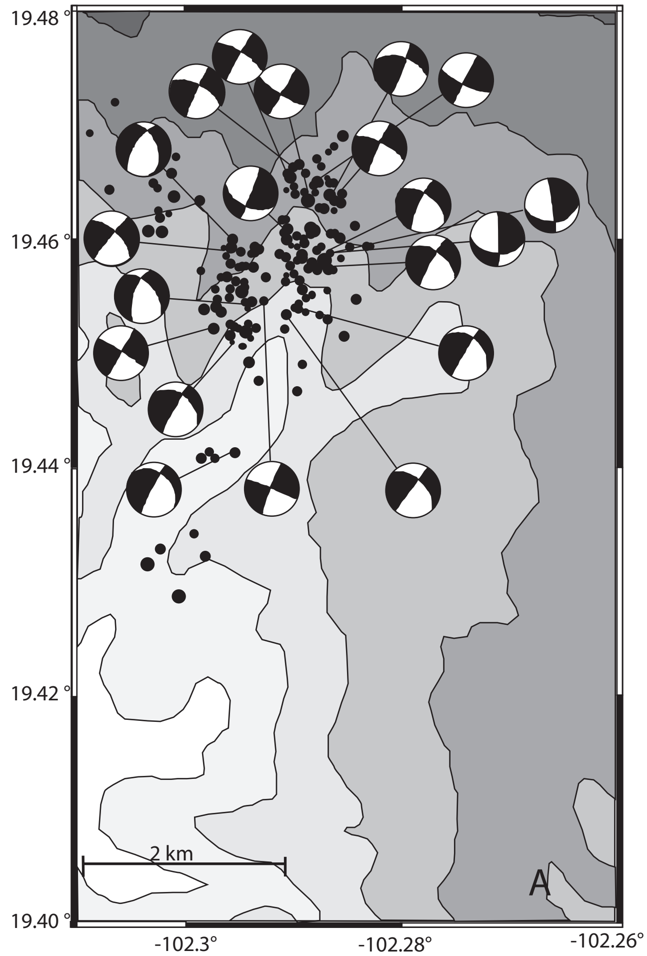

Figure 13. Focal Plane solutions for **(A)** a tectonic earthquake swarm from Central Mexico (modified from Pacheco et al., 1999) and **(B)** a magmatic earthquake swarm located in Southwestern Alaska near Iliamna Volcano (modified from Roman et al, 2004). Notice the similarity of focal mechanisms for **(A)** the tectonic swarm, compared to the variation found in **(B)** the magmatic swarm.

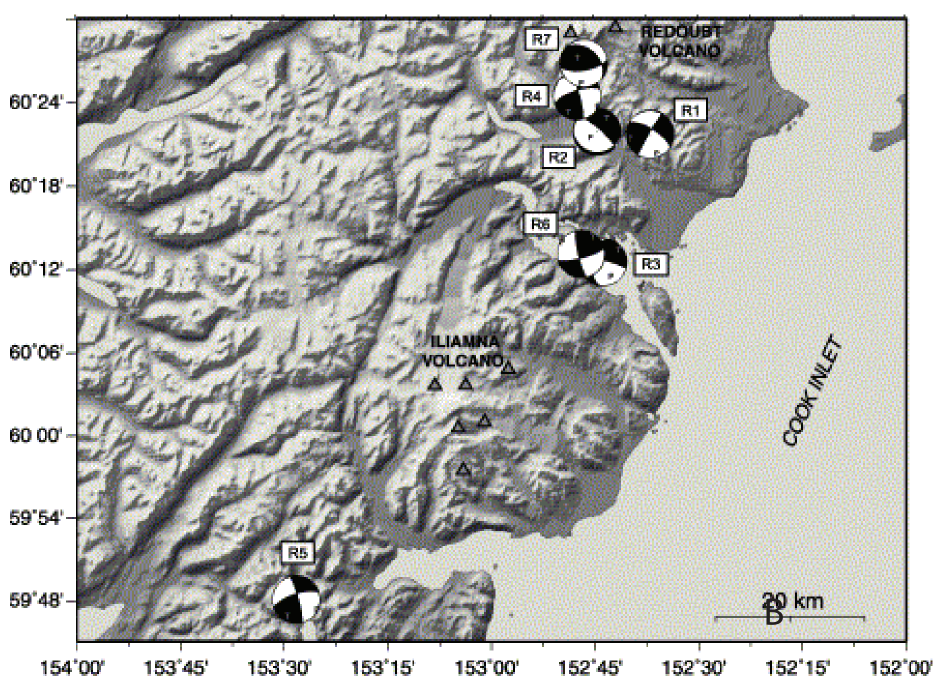

This magmatic event represents what I believe to be a dike intruding into the crust (Fig. 14). In connecting the dike behavior to the hypocenter behavior, I have separated the intrusion into three stages which correlate to the stages discussed in Figure 5.

In Stage I, the magma began its ascent, starting at a depth of approximately 9 km (Fig. 14A). Gas and fluid present at the top of the dike helped drive fracturing, by causing stress to accumulate. Once the stress accumulation reached a critical point, a fracture opened, and allowed the dike to inject itself upwards.

In Stage II the dike slowly ascended from 9 km to approximately 5 km depth, while also migrating laterally to the north (Fig. 14B). The ascent of the magma terminated at this depth, and for a short time, the migration paused before the onset of Stage III. This is most likely due to the dike reaching a layer within the crust where the driving mechanism was no longer dominant.

During Stage III, magma build-up continued, resulting in a lateral extension of the system (Fig. 14C). Magma, remaining at a depth of 5km, migrated back to the southeast over a period of three weeks. At this point, the swarm terminated and migratory behavior is assumed to halt.

CONCLUSIONS

This study examined the behavior of a seismic swarm observed during June 2006 in the Michoacan-Guanajuato volcanic field. Due to its location and the initial examination of hypocenters, the swarm could be interpreted as either tectonic or

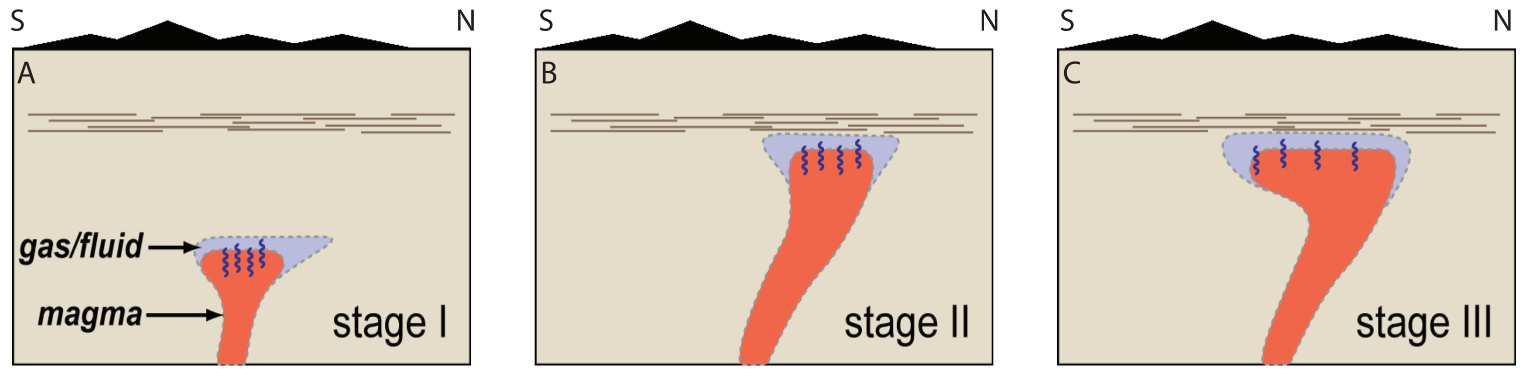

Figure 14. Schematic model of possible dike migration. This is also split into three stages, analagous to Figure 5, corresponding the migratory motion of the swarm with the ascent of the intrusion.

magmatic. Because of extensive analysis done with spatial and temporal trends as well as focal mechanism solutions, I interpret this swarm to be magmatic. The combination of the migratory behavior of the hypocenters and the inconsistency of focal mechanisms are indicative of a possible dike emplacement occurring during this time period.

ACKNOWLEDGEMENTS

This study was funded by the Incorporated Research Institutions of Seismology (IRIS) Summer Internship Program. Data from the arrays were provided by the University of Texas Austin, New Mexico State University in conjunction with Instituto de Geofisica, UNAM (MARS), the University of Alaska Fairbanks (CODEX), and the Volcanic Observatory at the Universidad de Colima. I also thank Matt Gardine and Mike West for their contributions and suggestions during the initial processing and analysis of the data, and Sarah Titus for her insight and suggestions during the writing and editing of this paper.

REFERENCES CITED

Brown, J., Prejean, S. G., Zhang, H., Power, J., and Anonymous, 2004, Double difference earthquake relocation and tomography at Mount Spurr Volcano, Alaska, 1991 to 2004: Washington, American Geophysical Union.

Cronin, V. S., 2004, A draft primer on focal mechanism solutions for geologists: Teaching Quantitative Skills in the Geosciences: (last accessed March, 9)

Dunn, M., Horton, S., Deshon, H., Powell, C., and Scharnberger, C., 2008, HypoDD relocation of earthquakes in the New Madrid seismic zone, Seismological Research Letters: El Cerrito, Seismological Society of America, p. 137.

Ferrari, L., Conticelli, S., Vaggelli, G., Petrone, C. M., and Manetti, P., 2000, Late Miocene volcanism and intra-arc tectonics during the early development of the Trans-Mexican Volcanic Belt: Tectonophysics, v. 318, p. 161-185.

Ferrari, L., Garduno, V. H., Innocenti, F., Manetti, P., Pasquare, G., and Vaggelli, G., 1994, A widespread mafic volcanic unit at the base of the Mexican Volcanic Belt between Gudalajara and Queretaro: Geofisica Internacional, v. 33.

Frohlich, C., 1994, Earthquakes with Non-Double-Couple Mechanisms: Science, v. 264, p. 804-809.

Frohlich, C., Riedesel, M. A., and Apperson, K. D., 1989, Note Concerning Possible Mechanisms for Non-Double-Couple Earthquake Sources: Geophysical Research Letters, v. 16, p. 523-526.

Gardine, M. D., Dominguez, T., West, M. E., Grand, S. P., and Suhardja, S. K., 2007, The Deep Seismic Structure of Volcan de colima: AGU Spring Meeting Abstracts, p. A2+.

Gomez-Tuena, A., Orozco-Esquivel, M. T., and Ferrari, L., 2007, Igneous petrogenesis of the Trans-Mexican volcanic belt, *in* Alaniz-Alvarez, S. A., and Nieto-Samaniego, A. F., eds., Geology of Mexico: Celebrating the Centenary of the Geological Society of Mexico, Geological Society of America Special Paper 422, p. 129-181.

Grand, S. P., Yang, T., Wilson, D., Guzman Speziale, M., Gomez Gonzales, J., Dominguez Reyes, T., and Ni, J., 2007, The seismic structire of the Rivera subduction zone: AGU Fall Meeting Abstracts, p. C702+.

Hasenka, T., and Carmichael, I., 1985, The cinder cones of Michoacan-Guanajuato,central Mexico: their age, volume, distribution, and magma discharge rate: Journal of Volcanology and Geothermal Research, v. 25, p. 105-124.

Hill, D. P., 1977, A model for earthquake swarms: Journal of Geophysical Research, v. 82, p. 1347-1352.

Hill, D. P., Ellsworth, W. L., Johnston, M. J. S., Langbein, D. H., Oppenheimer, D., Pitt, A. M., Reasenberg, P., Sorey, M. L., and McNutt, S. R., 1990, The 1989 earthquake swarm beneath Mammoth Mountain, California: an initial look at the 4 May through 30 September activity: Bulletin of the Seismological Society of America, v. 80, p. 325-339.

Ibs-von Seht, M., Plenefisch, T., and Klinge, K., 2008, Earthquake swarms in continental rifts -- A comparison of selected cases in America, Africa and Europe: Tectonophysics, v. 452, p. 66-77.

Kanamori, H., 1981, The nature of seismicity patterns before large earthquakes, *in* Simpson, W., and Rishards, P. G., eds., Earthquake Prediction: Washingon DC, American Geophysical Union, p. 1-19.

Kiratzi, A., Sokos, E., Ganas, A., Tselentis, A., Benetatos, C., Roumelioti, Z., Serpetsidaki, A., Andriopoulos, G., Galanis, O., and Petrou, P., 2008, The April 2007 earthquake swarm near Lake Trichonis and implications for active tectonics in western Greece: Tectonophysics, v. 452, p. 51-65.

Krauskopf, K. B., 1948, Mechanism of eruption at Paricutin Volcano, Mexico Bulletin of the Geological Society of America, v. 59, p. 711-732.

Legrand, D., Calahorrano, A., Guillier, B., Rivera, L., Ruiz, M., Villagómez, D., and Yepes, H., 2002, Stress tensor analysis of the 1998-1999 tectonic swarm of northern Quito related to the volcanic swarm of Guagua Pichincha volcano, Ecuador: Tectonophysics, v. 344, p. 15-36.

Luhr, J. F., Nelson, S. A., Allan, J. F., and Carmichael, I. S. E., 1985, Active rifting in southwestern Mexico: Manifestations of an incipient eastward spreading-ridge jump: Geology, v. 13, p. 54-57.

Macias, J. L., 2007, Geology and eruptive history of some active volcanoes, *in* Alaniz-Alvarez, S. A., and Nieto-Samaniego, A. F., eds., Geology of Mexico: Celebrating the Centenary of the Geological Society of Mexico, Geological Society of America Special Paper 422, p. 183-232.

Mandal, P., and Horton, S., 2007, Relocation of aftershocks, focal mechanisms and stress inversion; implications toward the seismotectonics of the causative fault zone of Mw7.6 2001 Bhuj earthquake (India): Tectonophysics, v. 429, p. 61-78.

Miller, A. D., Foulger, G. R., and Julian, B. R., 1998, Non-double-couple earthquakes: observations: Reviews of Geophysics, v. 36, p. 551-568.

Mogi, K., 1963, Some Discussions on Aftershocks, Foreshocks, and Earthquake Swarms: the Fracture of a Semi-infinite Body Caused by an Inner stress Origin and Its Relation to Earthquake Phenomena: Bulletin of the Earthquake Research Institute = Tokyo Daigaku Jishin Kenkyusho Iho, v. 41, p. 615-658.

Moore, G., Marone, C., Carmichael, I., and Renne, P., 1994, Basaltic volcanism and extension near the intersection of the Sierra Madre volcanic province and the Mexican Volcanic Belt: Geological Society of America Bulletin, v. 106, p. 383-394.

Nettles, M., and Ekstrom, G., 1998, Faulting mechanism of analagous earthquakes near Bardarbunga Volcano, Iceland: Journal of Geophysical Research, v. 103, p. 17973-17983.

Newman, A. V., Dixon, T. H., Ofoegbu, G. I., and Dixon, J. E., 2001, Geodetic and seismic constraints on recent activity at Long Valley Caldera, California: evidence for viscoelastic rheology: Journal of Volcanology and Geothermal Research, v. 105, p. 183-206.

Pacheco, J. F., Mortera-Gutierrez, C. A., Delgado, H., Singh, S. K., Valenzuela, R. W., Shapiro, N. M., Santoyo, M. A., Hurtado, A., Barron, R., and Gutierrez-Moguel, E., 1999a, Tectonic significance of an earthquake sequence in the Zacoalco half-graben, Jalisco, Mexico: Journal of South American Earth Sciences, v. 12, p. 557-565.

Pacheco, J. F., Valdes-Gonzalez, C., Delgado, H., Singh, S. K., Zuniiga, F. R., Mortera-Gutierrez, C. A., Santoyo, M. A., Dominguez, J., and Barron, R., 1999b, Tectonic implications of the earthquake swarm of 1997 in the Michoacan Triangle, Mexico: Journal of South American Earth Sciences, v. 12, p. 567-577.

Pederson, R., Sigmundsson, F., and Einarsson, P., 2007, Controlling factorson earthquake swarms associated with magmatic intrusions: Journal of Volcanology and Geothermal Research, v. 162, p. 73-80.

Reasenberg, P., and Oppenheimer, D., 1985, FPFIT, FPPLOT, and FPPAGE: FORTRAN Computer Programs for Calculating and Displaying Earthquake Fault-plane Solutions, US Dept. of the Interior, Geolgical Survey.

Rikitake, T., 1975, Earthquake precursors: Bulletin of the Seismological Society of America, v. 65, p. 1133-1162.

Roman, D. C., Power, J. A., Moran, S. C., Cashman, K. V., Doukas, M. P., Neal, C. A., and Gerlach, T. M., 2004, Evidence for dike emplacement beneath Iliamna Volcano, Alaska in 1996: Journal of Volcanology and Geothermal Research, v. 130, p. 265-284.

Rosas-Elguera, J., Ferrari, L., Garduno-Monroy, V. H., and Urrutia-Fucugauchi, J., 1996, Continental boundaries of the Jalisco block and their influence in the Pliocene-Quaternary kinematics of western Mexico: Geology, v. 24, p. 921-924.

Shlien, S., and Nafi Toksoz, M., 1970, A clustering model for earthquake occurrences: Bulletin of the Seismological Society of America, v. 60, p. 1765-1787.

Stein, S., and Wysession, M., 2003, An Introduction to Seismology, Earthquakes, and Earth Structure: Malden, Blackwell Publishing.

Sykes, L. R., 1970, Earthquake swarms and sea-floor spreading: Journal of Geophysical Research, v. 75, p. 6598-6611.

Toda, S., Stein, R. S., and Sagiya, T., 2002, Evidence from the AD 2000 Izu Islands earthquake swarm that stressing rate governs seismicity: Nature, v. 419, p. 58-61.

von Seggern, D. H., Smith, K. D., and Preston, L. A., 2008, Seismic spatial-temporal character and effects of a deep (25-30 km) magma intrusion below north Lake Tahoe, California-Nevada: Bulletin of the Seismological Society of America, v. 98, p. 1508-1526.

Waldhauser, F., and Ellsworth, W. L., 2000, A Double-difference Earthquake Location Algorithm: Method and Application to the Northern Hayward Fault, California: Bulletin of the Seismological Society of America, v. 90, p. 1353-1368.